Proceedings of 14th IOE Graduate Conference
Peer Reviewed
Year: 2023 Month: December Volume: 14
ISSN: 2350-8914 (Online), 2350-8906 (Print)

Small Signal Stability of Parallel Connected Voltage Source Inverters

Nawaraj Poudel [a], Suraj Shrestha [b], Deependra Neupane [c]

[a, c] *Department of Electrical Engineering, Purwanchal Campus, Institute of Engineering, Tribhuvan University, Dharan, Nepal*
[b] *Department of Electrical Engineering, Paschimanchal Campus, Institute of Engineering, Tribhuvan University, Pokhara, Nepal*
[a] nawarajpoudel@ioepc.edu.np, [b] suraj@wrc.edu.np, [c] deependra@ioepc.edu.np

Abstract
For a variety of reasons, including the challenge of grid extension, standalone hybrid energy systems are an enticing option for electrifying remote areas. As a result, important fields of power system research have emerged around the idea of the microgrid and micro-grid control strategies. The island microgrid is made up of numerous power inverters and different kinds of power equipment. System instability may result from the interaction of inverters with various control strategies, which will lead to malfunctions in the power equipment. Therefore, in order to enable parallel operation while maintaining system stability, an appropriate control strategy must be implemented. The development of a mathematical model for parallel connected Voltage Source Inverters (VSI) using a traditional droop control strategy is the main goal of this study. The system's linear state space model has been constructed. The parameter sensitivity for the stability has been examined because the loading, controller, and system parameters all affect the small signal stability of the system. After that, the suggested model was constructed using MATLAB/SIMULINK, and the outcomes of electrical system simulation and mathematical modeling were contrasted. The sensitivity to controller gain parameters and the eigenvalue analysis have been examined. A 3 kVA linear load has been taken into consideration for a parallel inverter system. Additional load of 1 kVA have been added to study the system stability on load perturbation.

Keywords
VSI, Small Signal Stability, Parallel Operation

1. Introduction

The island microgrid is composed of many inverters and various types of power equipment, and the interaction between inverters with different control methods may cause system instability, which will cause the power equipment to malfunction [1]. Therefore, practical strategies for analyzing the stability of the microgrid system have become particularly important [2]. The influence of the control parameters on the system's behavior can be studied using the proposed state equation model, which will obtained from the small signal analysis. In islanded AC microgrids, three-phase droop-controlled inverters are widely employed as power interfaces of DGs [3]. Since the active power-frequency and reactive power-voltage amplitude droop control scheme is applied, automatic power sharing between parallel inverters can be achieved independent of communication [4]. However, the output impedance of the inverter plays and import role in power sharing in droop controlled inverters [5].

Several renewable energy-based distributed generators are operated in parallel through DC-AC converters with having individual control loops with various control strategies. Thus, the dynamic stability problem in microgrids becomes more significant due to many power converters. Power electronics system dynamic stability has been researched for a long time. Small-signal models are frequently used since it is crucial to understand how a system reacts to different changes. The dynamics characteristics and the intraction between the power electronic devices in the system are studied using small signal analysis. The study is done by synthesising the system around a specific operating point. In order to choose the control loop parameters, frequency domain or time domain methods are often used. This makes it a necessary and unavoidable task for system designers.

A systematic approach to petite signal modelling and control design of three-phase pwm inverters in early 1993 [6]. Similarly, the design of the output impedance of UPS inverters with parallel connection capability with small signal modelling have been performed in [5, 7]. An important contribution has been made on modeling and analysis of autonomous operation of inverter-based micro grids by modelling each sub module in state space and all combined in common reference frame [8]. The small signal modelling and analysis for parallel connected voltage source inverters in frequency domain have been performed in [9]. The small signal modelling of digitally controlled grid connected inverters with LCL filters [10, 11]. This study is based on the droop control method in microgrid. The small signal analysis of parallel connected voltage source inverters using frequency and voltage droop control, including an additional phase shift, has been studied on [12]. The small signal modelling of three three-phase isolated inverter with both voltage and frequency droop control [13]. Similarly, an accurate small single model of inverter-dominated islanded microgrids using a dq reference frame has been performed on [14].

The parallel-operated voltage source inverter small-signal model presented in this study can be utilized to construct the control loop and analyze the system's stability. The droop method has been widely used in the parallel operation of inverters. The coefficients of the droop controller and the gain of voltage and current loop controller influence the transient response and stability of the paralleled inverters system. This study have compared the results from the mathematical

modeling and that from the electrical simulation of actual system. Most of the study are focused on developing mathematical model and testing the system in real time or simulation basis. However, this study presents a comparison on the linear model and the simulation model side by side.

A mathematical model is presented in section II, where the variations in output d-q axis voltages and currents are taken into account as state variables, the variations in power inverter duty cycles and frequency are considered as the control input, and the variations in DC power source voltages are used as external disturbances. However, the effect of power source voltage has yet to be considered in the analysis. Linear model and Control strategy and a model of a general control system are discussed in subsection of section II. The results are analyzed in section III, beginning with the model verification, eigenvalue analysis, sensitive analysis and time domain simulation.

2. Methodology

First of all the methodological framework for this work was performed with the configuring the parallel inverters feeding the load is shown in figure 1. Figure 1 shows the two parallel inverters feeding load with individual coupling impedance. Individual VSI have their own voltage and current control loops with droop control strategy. The VSI consists of LC filter with couping reactance to connect in parallel. As usual the load in micro grid can vary, hence an additional load with a circuit breaker has been used.

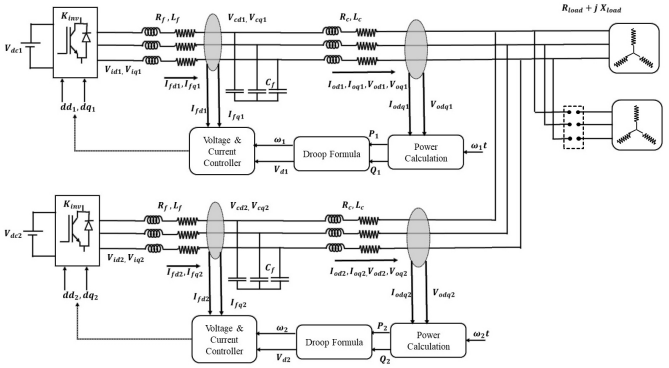

Figure 1: Parallel Inverter Connected with Load

2.1 Modelling of Parallel Inverters With Load

The coupling impedance and filter have the most contributions to the inverter dynamics. A set of differential equations given in equations 1 for voltage source inverter in the dq0 frame [15] can be used to represent the LC filter. Additionally, the inverter output provides the input voltage for the LC filter. A gain element can be used to represent the output voltage of the inverter in the dq0 frame of reference. Figure 1 displays the general schematic of the load-connected inverter system with an LC filter and a coupling impedance.

For Inverter I

$$\frac{d}{dt}\begin{bmatrix} I_{fd} \\ I_{fq} \end{bmatrix} = \begin{bmatrix} -\frac{R_f}{L_f} & \omega \\ -\omega & -\frac{R_f}{L_f} \end{bmatrix}\begin{bmatrix} I_{fd} \\ I_{fq} \end{bmatrix} + \frac{1}{L_f}\left(\begin{bmatrix} V_{id} \\ V_{iq} \end{bmatrix} - \begin{bmatrix} V_{cd} \\ V_{cq} \end{bmatrix}\right)$$
$$\frac{d}{dt}\begin{bmatrix} V_{cd} \\ V_{cq} \end{bmatrix} = \omega\begin{bmatrix} V_{cq} \\ V_{cd} \end{bmatrix} + \frac{1}{C_f}\left(\begin{bmatrix} I_{fd} \\ I_{fq} \end{bmatrix} - \begin{bmatrix} I_{od} \\ I_{oq} \end{bmatrix}\right) \quad (1)$$
$$\frac{d}{dt}\begin{bmatrix} I_{od} \\ I_{oq} \end{bmatrix} = \begin{bmatrix} -\frac{R_c}{L_c} & \omega \\ -\omega & -\frac{R_c}{L_c} \end{bmatrix}\begin{bmatrix} I_{od} \\ I_{oq} \end{bmatrix} + \frac{1}{L_c}\left(\begin{bmatrix} V_{cd} \\ V_{cq} \end{bmatrix} - \begin{bmatrix} V_{od} \\ V_{oq} \end{bmatrix}\right)$$

Where, R_f, L_f are filter resistance and inductance, C_f is filter capacitance and R_c, L_c are the common point side coupling resistance and inductance. I_{fd} and I_{fq} are dq component of inverterside current, V_{cd} and V_{cq} are the filter capacitance dq voltages and I_{od} and I_{oq} are the coupling reactor dq current. The dq represent vector of $[d1, q1], [d2, q2]$ for two inverters. These are the state variable of the inverter filter and couping reactance. The inverter is the combination of linear circuits with non linear switching devices. Nevertheless, the mathematical model of each individual switching circuit adds complexity to the system analysis. The switching portion of the inverter has been approximated in this study using the dq equivalent form. The duty cycle is used as the input in each frame to resolve the output from the inverter into the d and q frames. Equations give the inverter's output. The controlled duty cycle, V_{id} and V_{iq}, is used to generate the dq voltage output from the inverter.

$$V_{id1} = d_{d1}K_{inv}V_{dc1} \quad (2)$$
$$V_{iq1} = d_{q1}K_{inv}V_{dc1} \quad (3)$$
$$V_{id2} = d_{d2}K_{inv}V_{dc2} \quad (4)$$
$$V_{iq2} = d_{q2}K_{inv}V_{dc2} \quad (5)$$
$$(6)$$

where $d_{d1}, d_{q1}, d_{d2}, d_{q2}$ are the d_q equivalent of duty cycles. The duty cycle is obtained from the voltage control loop. V_{dc} is the input dc voltage, k_{inv} is duty cycle gain also called as Pulse Width Modulation (PWM) gain. The switching circuit of inverter have been represent as gain or first order system have been mentioned in several studies such as [16, 17, 18]. The small signal stability research in this work has ignored the dynamics of the inverter's switching and snubber circuits. However, MATLAB/SIMULINK has also been used to build the detailed model with switching circuits for the filter and inverter circuits. By linearising the large signal time average model around the specified beginning point, the small signal model of two parallel voltage source injectors may be derived.

2.2 Modelling of Load

According to Eq. (15) [8], the algebraic equation in the dq0 frame represents the relationship between the load's current and voltage.

$$\begin{aligned} V_{od} &= (i_{od1} + i_{od2})R_L - (i_{oq1} + i_{oq2})X_L \\ V_{oq} &= (i_{od1} + i_{od2})X_L + (i_{oq1} + i_{oq2})R_L \end{aligned} \quad (7)$$

$$\begin{aligned} P_{load} &= 1.5(V_{od}(i_{od1} + i_{od2}) + voqs((i_{oq1} + i_{oq2}))) \\ Q_{load} &= 1.5(V_{oq}(i_{od1} + i_{od2}) - vods((i_{oq1} + i_{oq2}))) \end{aligned} \quad (8)$$

where R_L and X_L are the load resistance and inductive reactance. Based on the load's active and reactive power, P_{load} and Q_{load}, respectively, R_L and X_L are computed. The load resistance and reactance at full loading are computed as

$$\begin{aligned} I_{nom} &= \frac{S_{base}}{\sqrt{3} \times V_{nom}} \\ R_L &= \frac{P_L}{3 \times I_{nom}^2} \\ X_L &= \frac{Q_L}{3 \times I_{nom}^2} \end{aligned} \tag{9}$$

where, S_{base} is rated system (addition of capacities of individual inverters) I_{nom} is nominal current for rated power, P_L and Q_L are the load active and reactive power. R_L and X_L are the equivalent load reistance and reactance for rated power.

2.3 Modelling of Controller

This study has taken the conventional droop control strategy for the inverters connected in parallel. Individual inverters are provided with voltage controller and current controller along with droop controller as shown in figure 2. The active and reactive power sharing between the inverters can be controlled by angular frequency and voltage magnitude difference between them. The angulare frequency is realted to active power sharing while the voltage magnitude is related to reactive power sharing. The angular frequency and reference voltage can be generated using the equation 10.

$$\begin{aligned} \omega_1 &= \omega_0 - m_1 \times P_1 \\ U_{dref1} &= V_{ref1} - n_1 \times Q_1 \\ \omega_2 &= \omega_0 - m_2 \times P_2 \\ U_{dref2} &= V_{ref2} - n_2 \times Q_2 \end{aligned} \tag{10}$$

where, V_{ref1} and V_{ref2} are the reference voltage of the system which equivalent to $V_{nom} \times \sqrt{\frac{2}{3}}$. Moreover, the m_1, m_2 are the active power droop coefficents and n_1, n_2 are the reactive power droop coefficent. Additionaly, P_1, P_2 are the active power measured and Q_1, Q_2 are the reactive power measured and can be calculated by using 11.

$$\begin{aligned} P_1 &= 1.5 \times (V_{cd1} I_{od1} + V_{cq1} I_{oq1}) \\ Q_1 &= 1.5 \times (V_{cd1} I_{oq1} - V_{cq1} I_{od1}) \\ P_2 &= 1.5 \times (V_{cd2} I_{od2} + V_{cq2} I_{oq2}) \\ Q_2 &= 1.5 \times (V_{cd2} I_{oq2} - V_{cq2} I_{od2}) \end{aligned} \tag{11}$$

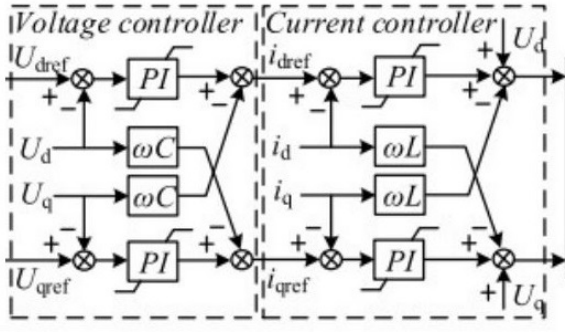

Figure 2: Block diagram of the droop control strategy adapted from [19]

2.3.1 Voltage Control Loop

The block diagram of voltage control loop is shown in above figure 2. This makes inverter output voltage reference tracking loop for output power given. It is responsible for maintaining system voltage. This control loop generates reference current signals which are supplied to the current control loop. For this output reference voltage (d component) from the droop controller is compared with the inverter output voltage and then the error is minimized by PI controller and then the obtained output is compared with inverter output I_{od} and $V_{cq}\omega Cf$. to generate reference current signal. Similar operation will occur for quadrature (q) component. The equation associated with voltage control loop are shown below:

$$\begin{aligned} i_{d1,ref} &= K_{pv1}(V_{ref,d1} - V_{cd1}) + K_{iv1}\int (V_{ref,d1} - V_{cd1})dt - \omega C_f V_{cd1} + I_{od} \\ i_{q1,ref} &= K_{pv1}(V_{ref,q1} - V_{cq1}) + K_{iv1}\int (V_{ref,q1} - V_{cq1})dt - \omega C_f V_{cq1} + I_{oq} \\ i_{d2,ref} &= K_{pv2}(V_{ref,d2} - V_{cd2}) + K_{iv2}\int (V_{ref,d2} - V_{cd2})dt - \omega C_f V_{cd2} + I_{od2} \\ i_{q2,ref} &= K_{pv2}(V_{ref,q2} - V_{cq2}) + K_{iv2}\int (V_{ref,q2} - V_{cq2})dt - \omega C_f V_{cq2} + I_{oq2} \end{aligned} \tag{12}$$

2.3.2 Current Control Loop

The block diagram of current control loop is shown in above figure. This improves dynamic response of system to enhance the system's anti-disturbance ability and provide even over current protection. This control loop generates reference voltage signal in dq form which are used as the reference signal in PWM after converting into abc frame. For this output reference current in (d) component from the current control loop is compared with the inverter output current and then the error is minimized by PI controller and then the obtained output is compared with inverter output V_{cd} and $I_{oq}\omega L_f$. to generate reference voltage signal. Similar action will occur for quadrature component. The equation associated with current control loop are shown below:

$$\begin{aligned} d_{d1} &= K_{pc1}(I_{d,ref1} - I_{fd1}) + K_{ic1}\int (I_{d,ref1} - I_{fd1})dt - \omega L_f I_{d,ref1} + V_{cd1} \\ d_{q1} &= K_{pc1}(I_{d,ref1} - I_{fd1}) + K_{ic1}\int (I_{d,ref1} - I_{fd1})dt - \omega L_f I_{q,ref1} + V_{cd1} \\ d_{d2} &= K_{pc2}(I_{d,ref2} - I_{fd2}) + K_{ic2}\int (I_{d,ref2} - I_{fd2})dt - \omega L_f I_{d,ref2} + V_{cd2} \\ d_{q2} &= K_{pc2}(I_{d,ref2} - I_{fd2}) + K_{ic2}\int (I_{d,ref2} - I_{fd2})dt - \omega L_f I_{q,ref2} + V_{cd2} \end{aligned} \tag{13}$$

2.4 Linearization and State Space Model

Small-signal stability is the outcome of the equation's linearization, which simplifies analysis under disturbance on the steady state or specific initial condition [20, 21]. Generally speaking, variations in loads and parameters (like the switching of small-capacity loads) are referred to as stochastic small disturbances. The stability analysis of a system with such small disturbances is often approximated by linear models due to the small stochastic excitation [22]. As a result, the linearized set of the equation simplifies the issue and aids in the creation of control plans.

2.4.1 Filter and Coupling Model

A generallized small signal model of a inverter is given as:

$$\frac{d}{dt}\begin{bmatrix}\Delta I_{fd}\\ \Delta I_{fq}\end{bmatrix} = \begin{bmatrix}-\frac{R_f}{L_f} & \Delta\omega\\ -\Delta\omega & -\frac{R_f}{L_f}\end{bmatrix}\begin{bmatrix}\Delta I_{fd}\\ \Delta I_{fq}\end{bmatrix} + \frac{1}{L_f}\left(\begin{bmatrix}\Delta V_{id}\\ \Delta V_{iq}\end{bmatrix} - \begin{bmatrix}\Delta V_{cd}\\ \Delta V_{cq}\end{bmatrix}\right)$$

$$\frac{d}{dt}\begin{bmatrix}\Delta V_{cd}\\ \Delta V_{cq}\end{bmatrix} = \omega\begin{bmatrix}\Delta V_{cq}\\ \Delta V_{cd}\end{bmatrix} + \frac{1}{C_f}\left(\begin{bmatrix}\Delta I_{fd}\\ \Delta I_{fq}\end{bmatrix} - \begin{bmatrix}\Delta I_{od}\\ \Delta I_{oq}\end{bmatrix}\right)$$

$$\frac{d}{dt}\begin{bmatrix}\Delta I_{od}\\ \Delta I_{oq}\end{bmatrix} = \begin{bmatrix}-\frac{R_c}{L_c} & \Delta\omega\\ -\Delta\omega & -\frac{R_c}{L_c}\end{bmatrix}\begin{bmatrix}\Delta I_{od}\\ \Delta I_{oq}\end{bmatrix} + \frac{1}{L_c}\left(\begin{bmatrix}\Delta V_{cd}\\ \Delta V_{cq}\end{bmatrix} - \begin{bmatrix}\Delta V_{od}\\ \Delta V_{oq}\end{bmatrix}\right) \tag{14}$$

2.4.2 Droop Equation

$$\begin{aligned}\Delta\omega_1 &= -m_1\times\Delta P_1\\ \Delta U_{dref1} &= -n_1\times\Delta Q_1\\ \Delta\omega_2 &= -m_2\times\Delta P_2\\ \Delta U_{dref2} &= -n_2\times\Delta Q_2\end{aligned} \tag{15}$$

2.4.3 Power Calculation

$$\begin{aligned}\Delta P_1 &= 1.5\times(\Delta V_{cd1}I_{od1} + V_{cd1}\Delta I_{od1} + \Delta V_{cq1}I_{oq1} + V_{cq1}\Delta I_{oq1})\\ \Delta Q_1 &= 1.5\times(\Delta V_{cd1}I_{oq1} + V_{cd1}\Delta I_{oq1} - \Delta V_{cq1}I_{od1} - V_{cq1}\Delta I_{od1})\\ \Delta P_2 &= 1.5\times(\Delta V_{cd2}I_{od2} + V_{cd2}\Delta I_{od2} + \Delta V_{cq2}I_{oq2} + V_{cq2}\Delta I_{oq2})\\ \Delta Q_2 &= 1.5\times(\Delta V_{cd2}I_{oq2} + V_{cd2}\Delta I_{oq2} - \Delta V_{cq2}I_{od2} - V_{cq2}\Delta I_{od2})\end{aligned} \tag{16}$$

2.4.4 Voltage and Current Controller

In Laplace domain, the linearized model of voltage and current control loop can be merged and can be given as:

$$\begin{aligned}\Delta d_{d1} &= \Delta V_{cd1} + H_{c1}(((V_{od,ref1} - \Delta V_{cd1})H_{v1} + \Delta i_{od1} - \Delta\omega_1 C_f V_{\Delta cq1}) - \Delta i_{fd1}) - \Delta\omega_1 L_f\Delta i_{fq1}\\ \Delta d_{q1} &= \Delta V_{cd1} + H_{c1}(((V_{od,ref1} - \Delta V_{cd1})H_{v1} + \Delta i_{od1} - \Delta\omega_1 C_f\Delta V_{cq1}) - \Delta i_{fd1}) - \Delta\omega_1 L_f\Delta i_{fq1}\\ \Delta d_{d2} &= \Delta V_{cd2} + H_{c2}(((\Delta V_{od,ref2} - \Delta V_{cd2})H_{v2} + \Delta i_{od2} - \Delta\omega_2 C_f\Delta V_{cq2}) - \Delta i_{fd2}) - \Delta\omega_2 L_f\Delta i_{fq2}\\ \Delta d_{q2} &= \Delta V_{cd2} + H_{c2}(((\Delta V_{od,ref2} - \Delta V_{cd2})H_{v2} + \Delta i_{od2} - \Delta\omega_2 C_f\Delta V_{cq2}) - \Delta i_{fd2}) - \Delta\omega_2 L_f\Delta i_{fq2}\end{aligned} \tag{17}$$

where, $H_{c1} = K_{pc1} + \frac{K_{ic1}}{s}$, $H_{c2} = K_{pc2} + \frac{K_{ic2}}{s}$, $H_{v1} = K_{pv1} + \frac{K_{iv1}}{s}$ and $H_{v2} = K_{pv2} + \frac{K_{iv2}}{s}$.

2.4.5 Open Loop Model

The set of differential algebraic equations mentioned in 14,16 and 15 can be represented in state space equation given as:

$$\begin{aligned}\dot{\Delta x} &= A_s\Delta x + B_s\Delta u + F_s\Delta v\\ \Delta y &= C_s\Delta x + D_s\Delta u\end{aligned} \tag{18}$$

where x is state variable vector, u is input vector and v is the other input vector, mainly disturbance input. The state variable vector for the parallel inveter is given as:

$$\Delta x = [\ \Delta i_{fd1}\quad \Delta i_{fq1}\quad \Delta v_{cd1}\quad \Delta v_{cq1}\quad \Delta i_{od1}\quad \Delta ioq_1\quad \Delta i_{fd2}\quad \Delta i_{fq2}\quad \Delta v_{cd2}\quad \Delta v_{cq2}\quad \Delta i_{od2}\quad \Delta ioq_2\ ]$$

$$\Delta u = [\Delta d_{d1}\quad \Delta d_{q1}\quad \Delta d_{d2}\quad \Delta d_{q2}]$$

$$\Delta v = [V_{dc1}V_{dc2}]$$

where, $A = \frac{\partial\dot{x}}{\partial x}, B = \frac{\partial\dot{x}}{\partial u}, C = \frac{\partial\dot{x}}{\partial v}$ at $x = x_0$ respectively. where x_0 is the point of linerization. The subsript 1 represents the state variables of inveter one and subscript 2 represents the state variable of inveter two. The A matrix can be obtained by differentiating the equations 1 with state vector. The A matrix is given as:

$$A = \begin{bmatrix}
-\frac{R_f}{L_f} & \omega_1 & -\frac{1}{L_f} & 0 & 0 & 0 & 0 & 0 & 0 & 0 & 0 & 0\\
-\omega_1 & -\frac{R_f}{L_f} & 0 & -\frac{1}{L_f} & 0 & 0 & 0 & 0 & 0 & 0 & 0 & 0\\
\frac{1}{C_f} & 0 & 0 & \omega_1 & -\frac{1}{C_f} & 0 & 0 & 0 & 0 & 0 & 0 & 0\\
0 & \frac{1}{C_f} & -\omega_1 & 0 & 0 & -\frac{1}{C_f} & 0 & 0 & 0 & 0 & 0 & 0\\
0 & 0 & \frac{1}{L_c} & 0 & -\frac{R_L}{L_c}-\frac{R_c}{L_c} & \omega_1+\frac{X_L}{L_c} & 0 & 0 & 0 & 0 & -\frac{R_L}{L_c} & \frac{X_L}{L_c}\\
0 & 0 & 0 & \frac{1}{L_c} & -\omega_1-\frac{X_L}{L_c} & -\frac{R_L}{L_c}-\frac{R_c}{L_c} & 0 & 0 & 0 & 0 & -\frac{X_L}{L_c} & -\frac{R_L}{L_c}\\
0 & 0 & 0 & 0 & 0 & 0 & -\frac{R_f}{L_f} & \omega_2 & -\frac{1}{L_f} & 0 & 0 & 0\\
0 & 0 & 0 & 0 & 0 & 0 & -\omega_2 & -\frac{R_f}{L_f} & 0 & -\frac{1}{L_f} & 0 & 0\\
0 & 0 & 0 & 0 & 0 & 0 & \frac{1}{C_f} & 0 & 0 & \omega_2 & -\frac{1}{C_f} & 0\\
0 & 0 & 0 & 0 & 0 & 0 & 0 & \frac{1}{C_f} & -\omega_2 & 0 & 0 & -\frac{1}{C_f}\\
0 & 0 & 0 & 0 & -\frac{R_L}{L_c} & \frac{X_L}{L_c} & 0 & 0 & \frac{1}{L_c} & 0 & -\frac{R_L}{L_c}-\frac{R_c}{L_c} & \omega_2+\frac{X_L}{L_c}\\
0 & 0 & 0 & 0 & -\frac{X_L}{L_c} & -\frac{R_L}{L_c} & 0 & 0 & 0 & \frac{1}{L_c} & -\omega_2-\frac{X_L}{L_c} & -\frac{R_L}{L_c}-\frac{R_c}{L_c}
\end{bmatrix}$$

The B matrix is given as:

$$B = \begin{bmatrix}
\frac{K_{inv}V_{dc1}}{L_f} & 0 & 0 & 0\\
0 & \frac{K_{inv}V_{dc1}}{L_f} & 0 & 0\\
0 & 0 & 0 & 0\\
0 & 0 & 0 & 0\\
0 & 0 & 0 & 0\\
0 & 0 & 0 & 0\\
0 & 0 & \frac{K_{inv}V_{dc1}}{L_f} & 0\\
0 & 0 & 0 & \frac{K_{inv}V_{dc1}}{L_f}\\
0 & 0 & 0 & 0\\
0 & 0 & 0 & 0\\
0 & 0 & 0 & 0\\
0 & 0 & 0 & 0
\end{bmatrix}$$

This gives the open loop model of parallel inverter. The open loop eigen values defines the stability of open loop model of inverter. System eigenvalues can determine the small-signal stability study of the system at any operating point. The small-signal stability begins with finding the equilibrium or operating point where the differential equation system is linearized, and the state matrix is obtained. The eigenvalues are then obtained from the state matrix with equilibrium point, i.e., eigenvalues of A. By linearizing around an equilibrium point, the dynamics of a non-linear system can be described.

2.4.6 Closed Loop Model

The parallel connected inverter are individually controlled by the current controller and voltage controllers as mentioned in section 2.3. The control diagram for the linearized model of inverter and controller is shown as:

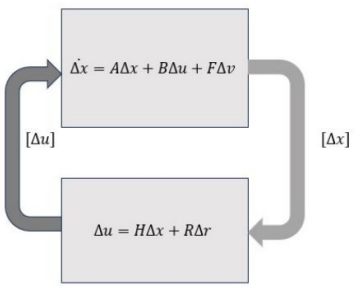

Figure 3: Control block of two parallel connected inverters

The linear equation represented by equations 17 can be written as:

$$U(s) = H(s)X_s(s) + J(s)R_c(s) \tag{19}$$

where, $X_s(s)$ gives the laplace transform of state variables and $R_c(s) = []$ The matrix H an R can be obtained as by rearranging the equation given by 17.

$$H^T = \begin{bmatrix} -H_{c1} & -L_f\omega_1 & 0 & 0 \\ -L_f\omega_1 & -H_{c1} & 0 & 0 \\ -H_{c1}H_{v1}+1 & C_fH_{c1}\omega_1 & 0 & 0 \\ -C_fH_{c1}\omega_1 & -H_{c1}H_{v1}+1 & 0 & 0 \\ H_{c1} & 0 & 0 & 0 \\ 0 & H_{c1} & 0 & 0 \\ 0 & 0 & -H_{c2} & -L_f\omega_2 \\ 0 & 0 & -L_f\omega_2 & -H_{c2} \\ 0 & 0 & -H_{c2}H_{v2}+1 & C_fH_{c2}\omega_2 \\ 0 & 0 & -C_fH_{c2}\omega_2 & -H_{c2}H_{v2}+1 \\ 0 & 0 & H_{c2} & 0 \\ 0 & 0 & 0 & H_{c2} \end{bmatrix} \tag{20}$$

$$J = \begin{bmatrix} H_{c1}H_{v1} & 0 \\ 0 & H_{c1}H_{v1} \\ H_{c2}H_{v2} & 0 \\ 0 & H_{c2}H_{v2} \end{bmatrix} \tag{21}$$

In order to build a compete closed loop model, the has to be merged. The state matrix given in 18 can be transformed to laplace domain as:

$$sX_s(s) = A_sX_s(s) + B_sU_s(s) + F_sV_s(s) \tag{22}$$

From equation 22 and 19, we can write:

$$sX_s(s) = A_sX_s(s) + B_s(H(s)X_s(s) + J(s)R_c(s)) + F_sV_s(s) \tag{23}$$

Taking, $V_s(s) = 0$, the transfer function can be written as:

$$\frac{X_s(s)}{R_c(s)} = \frac{B_sJ(s)}{sI - (A_s + B_sH_s)} \tag{24}$$

The characteristices equation for the overall closed system is given as:

$$P(s) = sI - (A_s + B_sH_s) \tag{25}$$

The solution of $P(s)$ gives the eigen values of the overall closed loop system.

2.5 Sensitivity and Stability Analysis

The system stability is defined by the Eigen value analysis of the state space model presented for the system given by equation 25. System eigenvalues can determine the small-signal stability study of the system at any operating point. The small signal stability begins with finding the equilibrium or operating point where the differential equation system is linearized, and the state matrix is obtained. The eigenvalues are then obtained from from solving the characteristics equation. The sensitivity analysis is performed by varying the controller parameters mainly gain of voltage controller K_{pv} and current controller K_{pc} on closed system.

The proposed system of equation i.e the transfer function given by 24 have been solved using the control system toolbox. The eigen values are obtained by solving the characteristics equation given in 25 using the solve function MATLAB. Moreover, the electrical system with actual switching devices has been modeled in SIMULINK and obtained the simulation result of the system.

3. Results

The proposed model have been analysed using eigen value analysis, frequency domain analysis and time domain simulation.Two parallel inverters system is adopted as an example, and the parameters of the system is listed in Table 2. The system and equation and the simulation have been performed for two different conditions viz. zero initial condition and a steady state condition. When the system reached to steady state condition, additional load of 100 kVA, 0.8 pf will be added in the system. The additional load will be proportionally shared by two inverters. While analysing the effect of load pertubation, eigen value analysis for the lineraztion point is given in Table 1.

Table 1: Point of linearization

Inverter I						
State Variable	Ifd1	Ifq1	Vcd1	Vcq1	Iod1	Ioq1
Value	1.393	3.4699	326.355	0	1.393	-1.65
Inverter II						
State Variable	Ifd1	Ifq1	Vcd1	Vcq1	Iod1	Ioq1
Value	3.496179	3.1119	326.49	0	3.4961	-2.016

Table 2: Parameter Used in Analysis

Parameter	**Value**	**Parameter**	**Value**
V_{nom}	400 V	I_{nom}	$\frac{P_{base}}{\sqrt{3}\times V_{nom}}$
P_{base}	3000 W	R_L	$\frac{P_{load}}{3\times I_{nom}^2}$
ω	377 $rads^{-1}$	X_L	$\frac{Q_{load}}{3\times I_{nom}^2}$
L_f	0.1 H	K_{inv}	0.01
C_f	1×10^{-4} F	P_{Load}	2400 W
L_c	0.00125 H	Q_{load}	1800 Var
R_c	0.01 Ω	K_{pv}	0.577
R_f	0.5 Ω	K_{iv}	1189.69
m	5×10^{-5}	K_{pc}	1570.79
n	3×10^{-5}	K_{ic}	157.07

3.1 Eigen Values and Sensitivity Analysis

The roots of the closed loop characteristics equations using the initial point of linearization gives the eigen values of the system. The eigen values gives the dynamics of system for any disturbance in the system. Figure 4 shows the location of eigen values in s-plane. The list of real and imaginary values of the

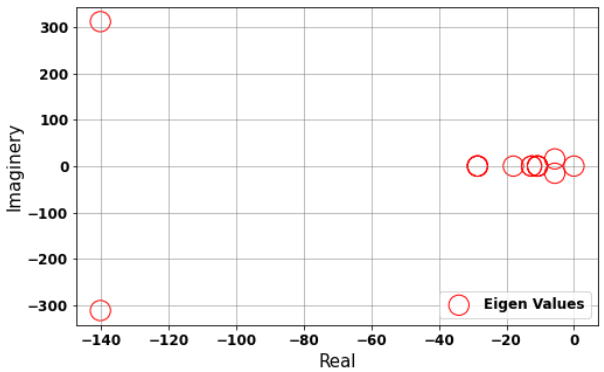

Figure 4: Dominant Closed Loop eigen values for Parallel Inverter Connected with Load

system is given in Table 3.

Table 3: Eigen Values of the closed loop system

S.N	Real Value	Imaginery Values
λ_1	-140.173258	±311.86
λ_1	-5.7820802	±13.04
λ_1	-17.92	0
λ_1	-12.5663	0
λ_1	-10.8193	0
λ_1	-28.57	0
λ_1	0	0

The dynamical characteristics of the proposed parallel inverter corresponds to an eigen values of the system. The free response of the parallel inverter can be obtained by a linear combination of the oscillatory modes determined by the eigen values [23]. Theoretically, the obtained eigen values can also appeared as very small values due to computational errors which are written as zero.

Figure 4 shows the eigen values of the two parallel inverters. The result shows that the system is stable in parallel connection as all the eigen values lie on the left hand side of s-plane. As the dominant eigen value consists of imaginery or complex roots results in parallel operation oscillatory. This is caused due to the power exchange between two parallel inverters as the dynamics of one of the inverter effect on the dynamics of other. The variation in the controller or system parameter in any one other inverter system may cause the system unstable. The variation in system or contorlller parameter cause shift in eigen value loacation. In this study, the controller parameter $K_{pv}, K_{iv}, K_{pc}, K_{ic}$ have been varied for 20 percent that of nomial value used to observe the stability performance for parallel inverter. The sensitivity for the controller parameters has been shown in figure 5.

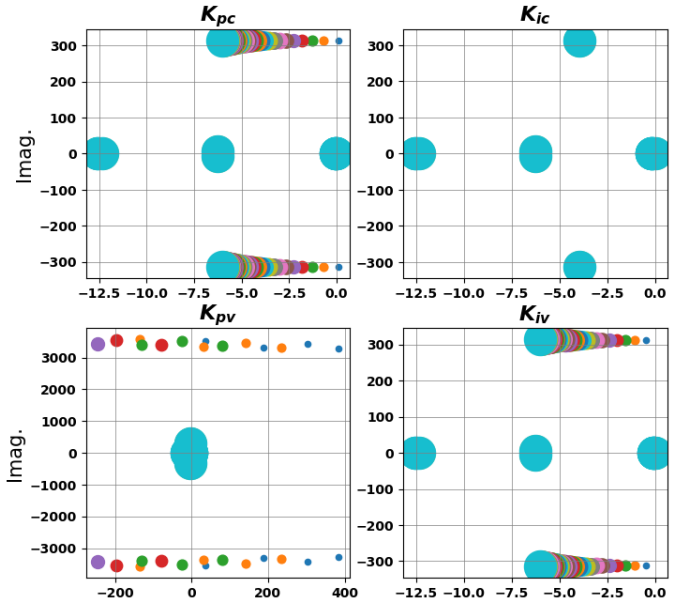

Figure 5: Dominant eigen values for Parallel Inverter Connected with Load for the variation of controller parameters

The stability range of the parallel inverter system and the variation of the eigenvalues have been determined by analyzing the eigenvalue trajectories. The system stability's sensitivity to the proportional and integral gain parameters of the voltage and current controllers, $K_{pv}, K_{iv}, K_{pc}, K_{ic}$, has been taken into account. With increasing circle size in Figure 5, the parameters become more noticeable. The dominant eigen values that lies near the imaginery line of s plane possess the most contribution in system dynamics. As a result, the sensitivity analysis has only displayed the dominant eigen values. Unless specified otherwise, the parameter set from Table 2 is used. As figure 5 illustrates, the system is intrinsically stable within a specific voltage gain parameter range, but becomes unstable at lower and even higher values of K_{pv}. As the parameter value increases, the eigen values shift from the left side of the s-plane to the right side. As figure 5 illustrates, the system is relatively less stable (long term oscillation) for lower ranges of the current gain parameter, but more stable when the voltage gain parameter, K_{pv}, is kept constant. The left hand eigen values are changing.

3.2 Time Domain Simulation

To compare and verify the proposed parallel inverter model with the droop controlled mode, the system of equation, written as transfer function have been solved using inverse transform. Moreover, the detail model of the inverter with switching circuits are modelled in MATLAB/SIMULINK using the simscape libraries. The parameters used of the simulation is listed in table 2. Initially, the load of 3 kVA with 0.8 pf have been used and simulated for 1 second. At simulation time of 1 second extra load of 1 kVA with 0.8 pf have been added in system. The simulation runs for 2 seconds. The terminal voltage reference for the system is taken as 326 peak (equivalent to 400 V rms line to line).

3.2.1 For Zero Initial Condition

Initially, the simulation runs with zero initial condition. The inverters share the load proportionally as per the droop coefficents as shown in figure 6. The solution obtained from both of the framework (electrical simulation from simulink and linear simulation from inverse transfrom) are similar in nature in the context active power and frequency of system. However, the results slightly differs in voltage and reactive power sharing. The system reached to steady state condition after 0.4 seconds. The steady state load sharing from inverters are about 1700 and 700 Watts. The reactive load sharing is found to be 1200 and 700 Vars. The response for frequency and voltage is shown in figure 7.

3.2.2 For Steady State Condition

At simulation time of 1 seconds, an additional load or 1 kVA have been added. The mathematical model solution and simulink result for active and reactive power sharing is shown in figure 8. The variation of load result caused the inverter to share load proportionally. However, the linear model and simulink result slightly differs. This is due to the linear apporoximation of the non linear system of linear equations. The frequency and voltage of the system is shown in figure 9. The frequency and voltage of the system slightly dipped in response to the additional load in system.

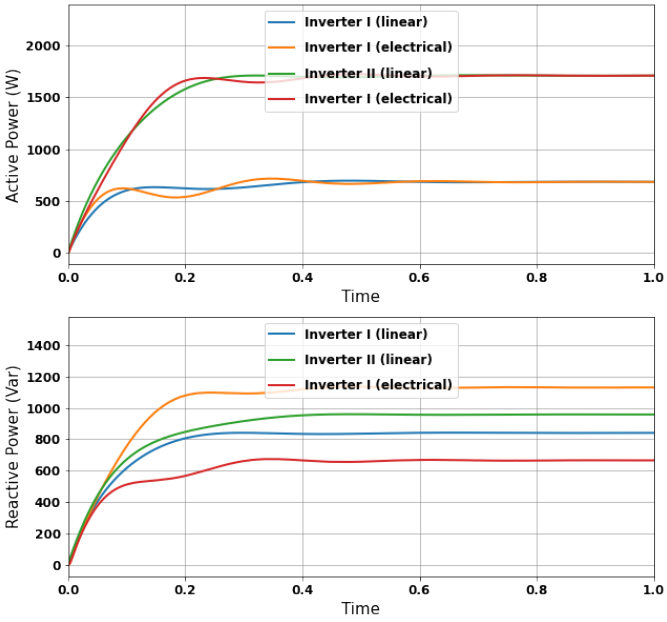

Figure 6: Active and Reactive power sharing between two inverters linear solution and SIMULINK result

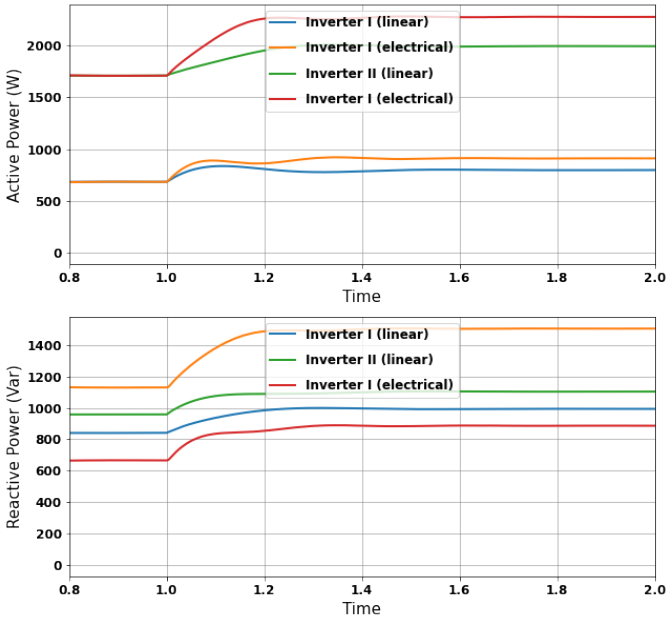

Figure 8: Active and reactive power sharing between inverters for the load variation at simulation time 1 second.

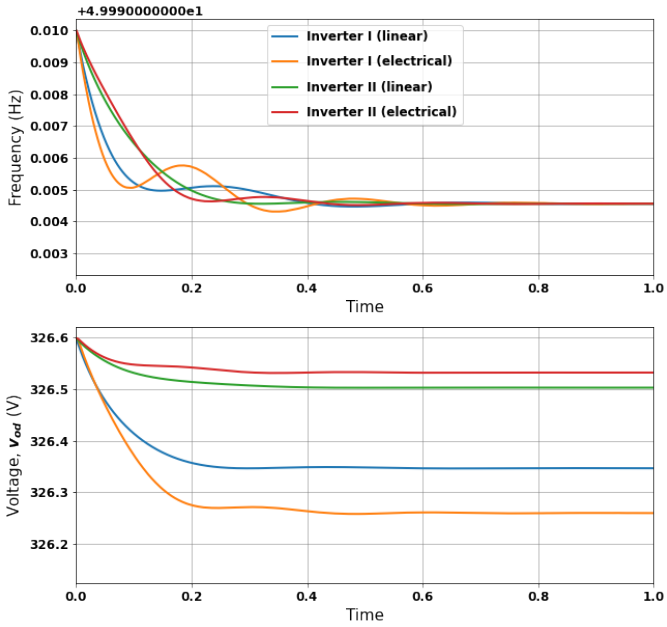

Figure 7: Angular frequency and terminal voltage of two inverters with linear solution and SIMULINK result

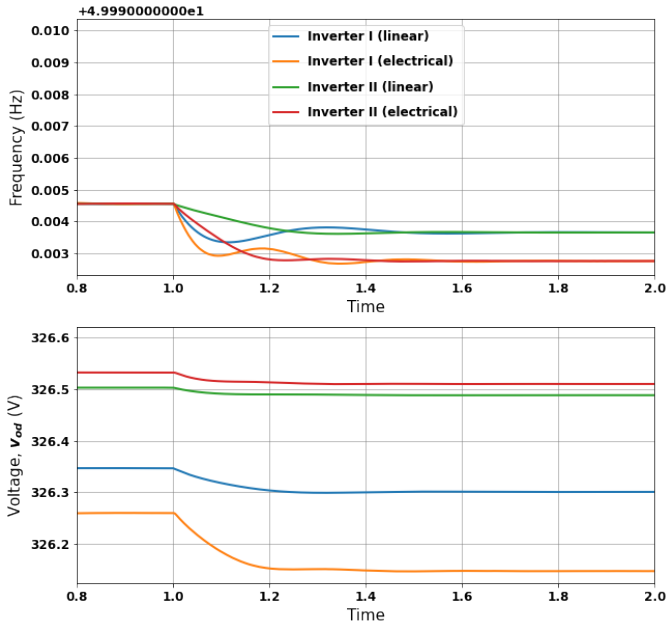

Figure 9: Frequency and voltage level of inveters for the load variation of 1 kVA at simulation time 1 sec

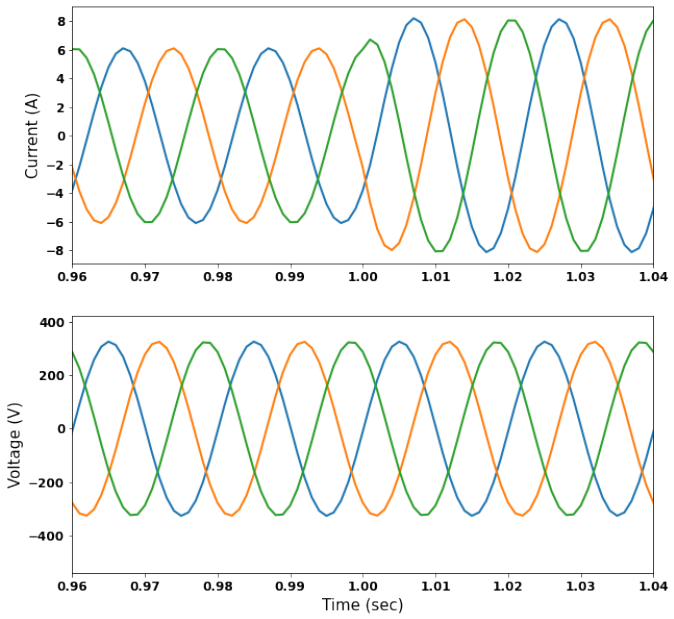

Figure 10: Instantaneous current and voltage waveform obtained from SIMULINK for load variation

The instantaneous wave-forms of voltage and current is shown in figure 10. The variation in load shows a smooth transition from 6 A peak to 8 A peak with slight disturbance.

4. Conclusion

This study have presented the small signal model of parallel connected inverters, performing the sensitivity analysis of control parameters for maximum stability. The model can be used to design the control loop and to study the system stability. The small signal model of the inverter takes the filter current and voltage and coupling reactance current as state variables. These variables are than utilized by current and voltage loop controllers. Two parallel inverter with different droop coefficient values have been used. The result shows the proportional sharing of load. The study is performed for both zero initial condition and load perturbation in steady state condition. The proposed mathematical models are used to determine the eigen values at steady state points. Moreover, the models are solved and the results are compared to that from the actual system realized in simulink. Additionally, from the study, we found that the controller parameter greatly influence on the stability and performance. This study has develop a framework to develop mathematical models of parallel connected inverter which may help in deriving more complex control strategies in future works.

Acknowledgments

The authors gratefully acknowledge Assoc. Prof. Bhrigu Bhattarai, Asst. Prof. Ram Prasad Pandey and Asst. Prof. Sandeep Dhami for their thoughtful critiques and recommendations.

References

[1] Bahador Fani, Ghazanfar Shahgholian, Hassan Haes Alhelou, and Pierluigi Siano. Inverter-based islanded microgrid: A review on technologies and control. *e-Prime-Advances in Electrical Engineering, Electronics and Energy*, page 100068, 2022.

[2] Xuan Zhang, Jinjun Liu, Zhiyuan You, and Linyuan Zhou. Small-signal analysis and modeling of parallel inverters based on the droop control method in micro-grid. In *2013 IEEE Energy Conversion Congress and Exposition*, pages 4580–4586. IEEE, 2013.

[3] Shike Wang, Zeng Liu, Jinjun Liu, Dushan Boroyevich, and Rolando Burgos. Small-signal modeling and stability prediction of parallel droop-controlled inverters based on terminal characteristics of individual inverters. *IEEE Transactions on Power Electronics*, 35(1):1045–1063, 2019.

[4] Josep M Guerrero, L Garcia De Vicuna, José Matas, Miguel Castilla, and Jaume Miret. A wireless controller to enhance dynamic performance of parallel inverters in distributed generation systems. *IEEE Transactions on power electronics*, 19(5):1205–1213, 2004.

[5] Josep M. Guerrero, Luis García De Vicuña, Jose Matas, Jaume Miret, and Miguel Castilla. Output impedance design of parallel-connected UPS inverters. *IEEE International Symposium on Industrial Electronics*, 2(4):1123–1128, 2004.

[6] Silva Hiti, Dushan Boroyevich, and Carlos Cuadros. Small-signal modeling and control of three-phase PWM converters. *Conference Record - IAS Annual Meeting (IEEE Industry Applications Society)*, 2(4):1143–1150, 1994.

[7] J. M. Guerrero, L. García De Vicuña, J. Miret, J. Matas, and J. Cruz. Output impedance performance for parallel operation of UPS inverters using wireless and average current-sharing controllers. *PESC Record - IEEE Annual Power Electronics Specialists Conference*, 4:2482–2488, 2004.

[8] Nagaraju Pogaku, Milan Prodanovic, and Timothy C Green. Modeling, analysis and testing of autonomous operation of an inverter-based microgrid. *IEEE Transactions on power electronics*, 22(2):613–625, 2007.

[9] Yu Zhang, Zhenhua Jiang, and Xunwei Yu. Small-signal modeling and analysis of parallel-connected voltage source inverters. In *2009 IEEE 6th International Power Electronics and Motion Control Conference, IPEMC '09*, volume 3, pages 377–383, 2009.

[10] Xiaotian Zhang, Joseph W. Spencer, and Josep M. Guerrero. Small-signal modeling of digitally controlled grid-connected inverters with LCL filters. *IEEE Transactions on Industrial Electronics*, 60(9):3752–3765, 2013.

[11] Xuan Zhang, Jinjun Liu, Zhiyuan You, and Linyuan Zhou. Small-signal analysis and modeling of parallel inverters based on the droop control method in micro-grid. *2013 IEEE Energy Conversion Congress and Exposition, ECCE 2013*, pages 4580–4586, 2013.

[12] Wanderley Alves Parreira, Henrique José Avelar, João Batista Vieira, Luiz Carlos Freitas, Luiz Carlos Gomes De Freitas, and Ernane Antônio Alves Coelho. Small-signal analysis of parallel connected voltage source inverters using a frequency and voltage droop control including an additional phase shift. *Journal of Control, Automation and Electrical Systems*, 25(5):597–607, 2014.

[13] Md Rasheduzzaman, Jacob Mueller, and Jonathan W. Kimball. Small-signal modeling of a three-phase isolated

inverter with both voltage and frequency droop control. *Conference Proceedings - IEEE Applied Power Electronics Conference and Exposition - APEC*, pages 1008–1015, 2014.

[14] Md Rasheduzzaman, Jacob A. Mueller, and Jonathan W. Kimball. An accurate small-signal model of inverter-dominated islanded microgrids using (dq) reference frame. *IEEE Journal of Emerging and Selected Topics in Power Electronics*, 2(4):1070–1080, 2014.

[15] Shengyang Lu, Yu Zhu, Lihu Dong, Guangyu Na, Yan Hao, Guanfeng Zhang, Wuyang Zhang, Shanshan Cheng, Junyou Yang, and Yuqiu Sui. Small-signal stability research of grid-connected virtual synchronous generators. *Energies*, 15(19):7158, 2022.

[16] Deependra Neupane and Nawaraj Poudel. Small-signal stability modeling, sensitivity analysis, and parameter optimization of improved virtual synchronous machine based standalone inverter. *Electric Power Components and Systems*, pages 1–17, 2023.

[17] Pawan Kumar Pathak, Anil Kumar Yadav, Sanjeevikumar Padmanaban, and PA Alvi. Design of robust multi-rating battery charger for charging station of electric vehicles via solar pv system. *Electric Power Components and Systems*, 50(14-15):751–761, 2022.

[18] Yoash Levron, Juri Belikov, and Dmitry Baimel. A tutorial on dynamics and control of power systems with distributed and renewable energy sources based on the dq0 transformation. *Applied Sciences*, 8(9):1661, 2018.

[19] Yiwen Geng, Lin Zhu, Xuanfeng Song, Kai Wang, and Xiaoqiang Li. A modified droop control for grid-connected inverters with improved stability in the fluctuation of grid frequency and voltage magnitude. *IEEE Access*, 7:75658–75669, 2019.

[20] Yuko Hirase, Kensho Abe, Kazushige Sugimoto, Kenichi Sakimoto, Hassan Bevrani, and Toshifumi Ise. A novel control approach for virtual synchronous generators to suppress frequency and voltage fluctuations in microgrids. *Applied Energy*, 210:699–710, 2018.

[21] Salvatore D'Arco, Jon Are Suul, and Olav B Fosso. Small-signal modelling and parametric sensitivity of a virtual synchronous machine. In *2014 Power Systems Computation Conference*, pages 1–9. IEEE, 2014.

[22] Lijuan Li, Yongdong Chen, Bin Zhou, Hongliang Liu, and Yongfei Liu. Linearization threshold condition and stability analysis of a stochastic dynamic model of one-machine infinite-bus (omib) power systems. *Protection and Control of Modern Power Systems*, 6:1–11, 2021.

[23] Prabha S Kundur and Om P Malik. *Power system stability and control*. McGraw-Hill Education, 2022.